https://doi.org/10.56295/1ACEG33

FINITE ELEMENT CHECK OF GSI ADJUSTMENT EQUATION RECONCILING HOEK-BROWN AND STEP-PATH STRENGTHS

Norbert R P Baczynski[1]; Alison McQuillan[2]
Prime Geotechnics Pty Ltd, Australia[1]; Rocscience, Australia[2]

ABSTRACT

Rock mass strength is impacted by the coalignment of geological defects and intact rock (IR) bridges. The greater the alignment of geological defects and smaller the rock bridges, the weaker the rock mass strength. Current versions of the 1980s Hoek-Brown Method (HBM) for rock mass strength considers rock mass blockiness and defect condition via a Geological Strength Index (GSI) chart. This chart was refined several times, but these revisions still do not directly consider coaligned defects and bridges. Step-Path Method (SPM) evolved in mid-1970s to assess strength implications of coaligned defects and IR bridges. Early SPM models were simple; but progressively evolved to consider more complex situations. In late 1980s, computer software was written to assess rock mass shear strength by Monte-Carlo statistical simulation of defect and IR bridge along failure paths through slopes. Since mid-2000s, EXCEL spreadsheets have aided this type of assessment. SPM often computes a lower rock mass strength than HBM. Based on 230+ case studies an equation was proposed in 2019 to adjust the GSI index in HBM based on relative occurrences of coaligned defects and IR bridges along failure paths. The general equation is $GSI_{Design} = \{GSI_{General\ Rock\ Mass} - [0.4 \times (\%\ coaligned\ defects)] + [1.2 \times (\%\ IR\ bridges)]\}$. With the above adjusted GSI, HBM computes near-same rock mass strength as SPM. Appropriateness of above GSI adjustment equation with respect coaligned defects is checked by two-dimensional (2D) jointed finite element (FE) modelling. Results are presented and discussed. The method is presented for alternative strength inputs into jointed rock masses to account for the presence of co-aligned defects dipping into the excavated slope.

Key words: Hoek-Brown, Step-Path, rock mass strength, GSI adjustment, finite element analyses

1 INTRODUCTION

Hoek-Brown (HBM) (Hoek and Brown, 1980) and Step-Path (SPM) (Jennings, 1970; Baczynski, 2000) methods assess rock mass (RM) shear strength. HBM considers rock mass blockiness and joint condition via a Geological Strength Index (GSI) chart. SPM considers the occurrence of coaligned defects and intact rock (IR) and/or rock mass (RM) bridges between these coaligned defects along potential failure path in slopes. Where coaligned defects are absent, HBM and SPM compute the same RM strength. As occurrence (%) of co-aligned defects increases, SPM strength progressively decreases until with 100% coaligned defect occurrence RM strength is same as coaligned defect strength. Thus, SPM strength is in between HBM strength and defect strength; yielding lower factors of safety (FOS) in limiting equilibrium analyses (LEA) of rock slope stability. Bar and Baczynski (2019) finite element modelled one slope case and inferred that SPM was a geotechnically logical approach. To reconcile differences between HBM and SPM rock mass strength estimates, Baczynski (2019) developed an GSI adjustment equation based on 230 case studies.

$$GSI_{Design} = \{GSI_{General\ Rock\ Mass} - [0.4 \times (\%\ coaligned\ defects)] + [1.2 \times (\%\ IR\ bridges)]\} \quad (1)$$

The 0.4 and 1.2 coefficients in this equation are generally applicable (correlation coefficients of 0.72 to 0.86); but they do somewhat vary (0.35-0.53 and 1.0-1.5) with rock type and mi (<11, 11-19 and >19) groupings respectively; with some groupings achieving better correlation coefficients of 0.98.

In this paper, the coaligned defects component of the GSI adjustment equation is checked by two-dimensional (2D) jointed finite element (FE) modelling. RS2 software (Rocscience, 2024) is used. Objectives, methodology, FE slope models, analysis results, conclusions and recommendations are presented and discussed. Baczynski (2019) suggested GSI adjustments due to intact rock bridges between coaligned defects was not investigated.

2 HOEK-BROWN METHOD

Hoek-Brown Method (HBM) for estimating rock mass strength was developed by Hoek and Brown (1980) and is now widely used. Inputs are unconfined compressive strength (UCS), shape of the triaxial strength curve (mi), rock mass blockiness and geological defect condition – estimated via the Geological Strength Index (GSI) chart (Hoek and Brown, 1997) and blasting disturbance (D). GSI is based on Bieniawski (1986, 1989) rock mass rating (RMR) index; but can also be estimated via Barton et al (1974) and other classifications, including Deere (1963) Rock Quality Designation (RQD). GSI chart was revised several times to make HBM better suited to specific ground situations; especially defect orientation in the rock mass. With respect to Step-Path Method (SPM), Truzman (2007) GSI chart is useful, if the term "intensity" is equated to "relative occurrence of geological defects that are coaligned with the failure path direction" (Baczynski, 2018). Figures 1 (a) and 1(b) show examples of two GSI charts.

3 STEP-PATH METHOD

Jennings (1970) detailed a basic Step-Path Method (SPM) for bedding planes failures in rock slopes. Since then, SPM has considered progressively more complex geotechnical conditions (Baczynski, 2000; Baczynski 2019). Although SPM is not widely used; it provides an approach to statistically quantify the extent to which geological defects coaligned with failure path direction and the IR / RM "bridges" between these defects contribute to RM shear strength. HBM strength is still assigned to those rock mass regions where coaligned defects do not statistically occur.

Figure 2 shows conceptual step-path methodology.

In Figure 2A, slope failure path complexity ranges from one set of coaligned defects to a composite situation. In the latter, the failure path traverses along a major backscarp fault, a central zone across the defect pattern and has HBM rock mass strength and then steps along short coaligned defects near slope toe. Figure 2B shows the three conceptual step-path "cell" types – coaligned defects, intact rock and rock mass.; with cells being shear-box tested individually and together. Figure 2C shows a multiple "cells" test; with anticipated shear strength dependent on relative occurrence of cell types. Figure 2D plots the expected shear strength relationship between the three cell types and SPM.

Strength relationship is intact rock > HBM rock mass > SPM rock mass > geological defect.

4 HBM-SPM 2019 RECONCILIATION

Baczynski (2019) reconciled HBM and SPM rock mass strength estimates by GSI adjustments; based on 230 case studies. Adjustments were computed via Microsoft EXCEL spreadsheet (Lambert and Frye, 2022) and ROCLAB-1.0 software (Rocscience, 2007).

Figure 3 (A to C) shows reconciliation plots for all rock types combined, sandstone and siltstone, respectively. As per 2019 paper, the method and adjustment equations are valid for GSI<75 and only yield sensible results when geological defects shear strength is less than HBM rock mass strength.

GSI adjustment Equation 1 for all rock types combined was presented in Section 1. Equations 2 and 3 are for sandstone (SS) and siltstone (SL) rock types, respectively.

$$GSI_{Design} = \{GSI_{SS\ Rock\ Mass} - [0.55 \times (\%\ SS\ coaligned\ defects)] + [1.0 \times (\%\ SS\ IR\ bridges)]\} \quad (2)$$

$$GSI_{Design} = \{GSI_{SL\ Rock\ Mass} - [0.41 \times (\%\ SL\ coaligned\ defects)] + [1.6 \times (\%\ SL\ IR\ bridges)]\} \quad (3)$$

Statistical correlation coefficients for the linear trends shown in Figure 3 range from 0.87 to 0.98.

5 FINITE ELEMENT MODELLING SOFTWARE

Modelling was done via RS2 two-dimensional (2D) jointed finite element (FE) software (Rocscience, 2020, 2024).

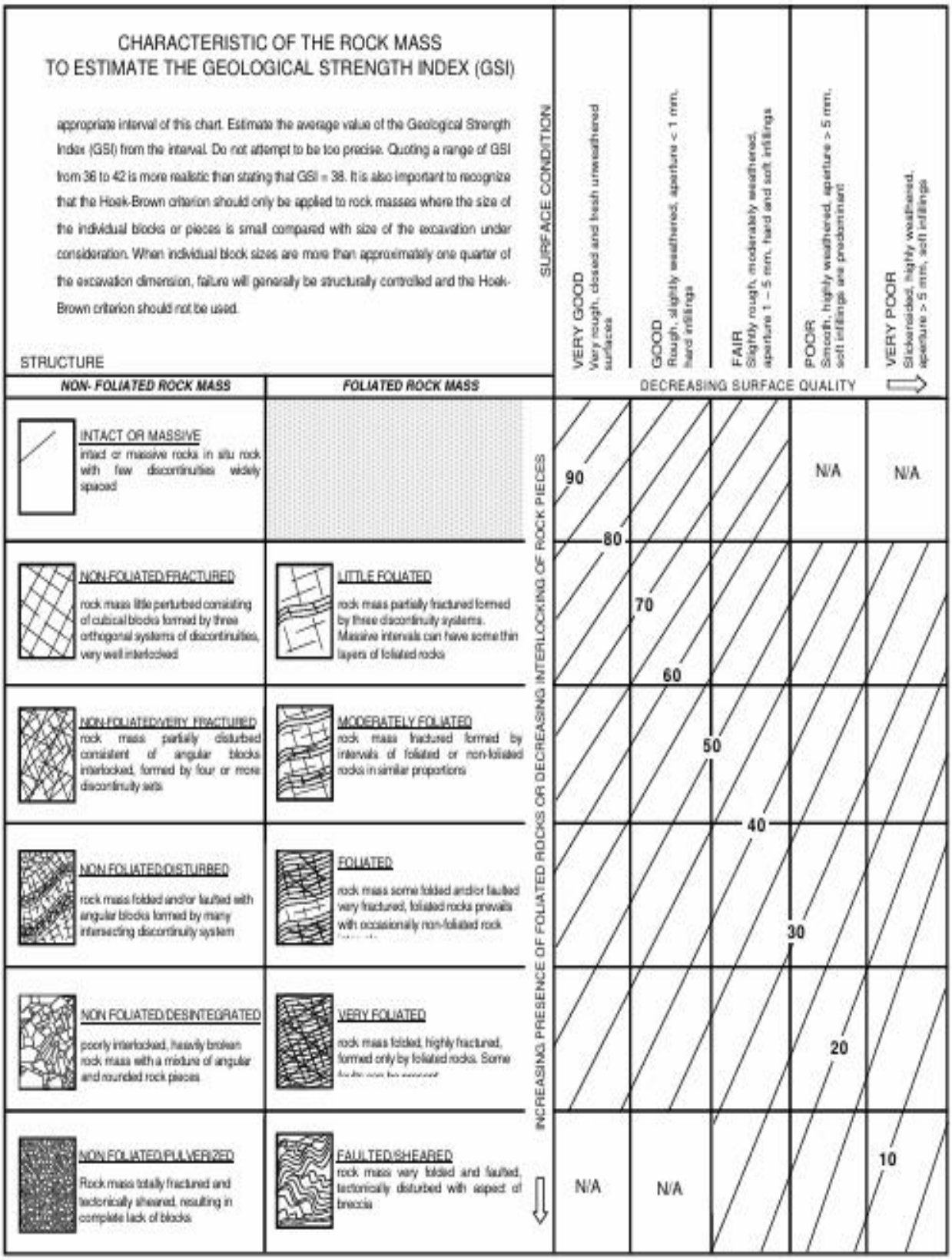

Figure 1(a): Truzman (2007) GSI chart

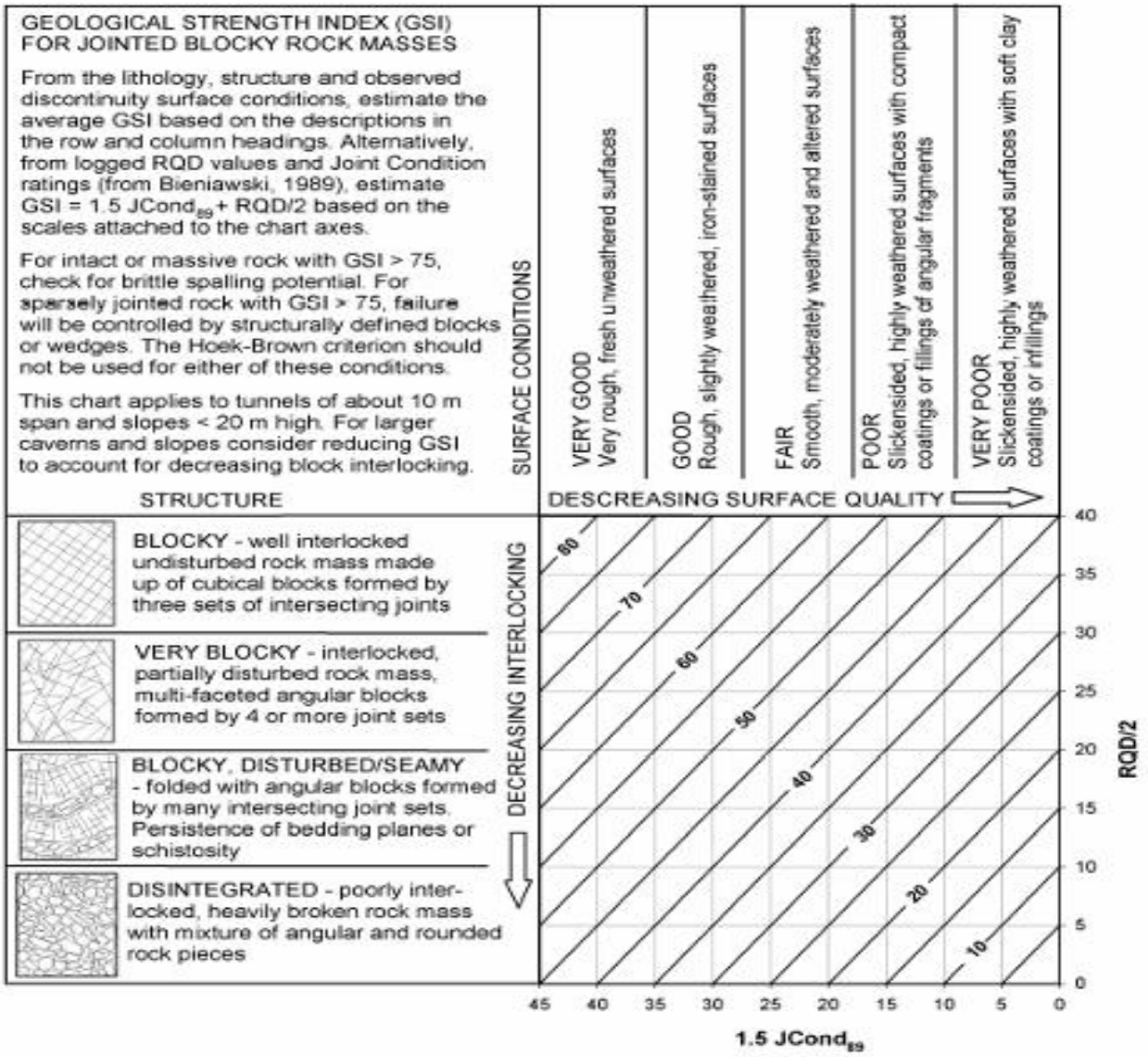

Condition of discontinuities	Very rough surfaces Not continuous No separation Unweathered wall rock	Slightly rough surfaces Separation < 1 mm Slightly weathered walls	Slightly rough surfaces Separation < 1 mm Highly weathered walls	Slickensided surfaces or Gouge < 5 mm thick or Separation 1 – 5 mm Continuous	Soft gouge > 5 mm thick or Separation > 5 mm Continuous
Rating	30	25	20	10	0

Guidelines for classification of discontinuity conditions

Discontinuity length (persistence) Rating	< 1 m 6	1 to 3 m 4	3 to10 m 2	10 to 20 m 1	More than 20 m 0
Separation (aperture) Rating	None 6	< 0.1 mm 5	0.1 – 1.0 mm 4	1 – 5 mm 1	More than 5 mm 0
Roughness Rating	Very rough 6	Rough 5	Slightly rough 3	Smooth 1	Slickensided 0
Infilling (gouge) Rating	None 6	Hard infilling < 5 mm 4	Hard filling > 5 mm 2	Soft infilling < 5 mm 2	Soft infilling > 5 mm 0
Weathering Rating	Unweathered 6	Slightly weathered 5	Moderate weathering 3	Highly weathered 1	Decomposed 0

Figure 1(b): Hoek et al (2013) GSI chart

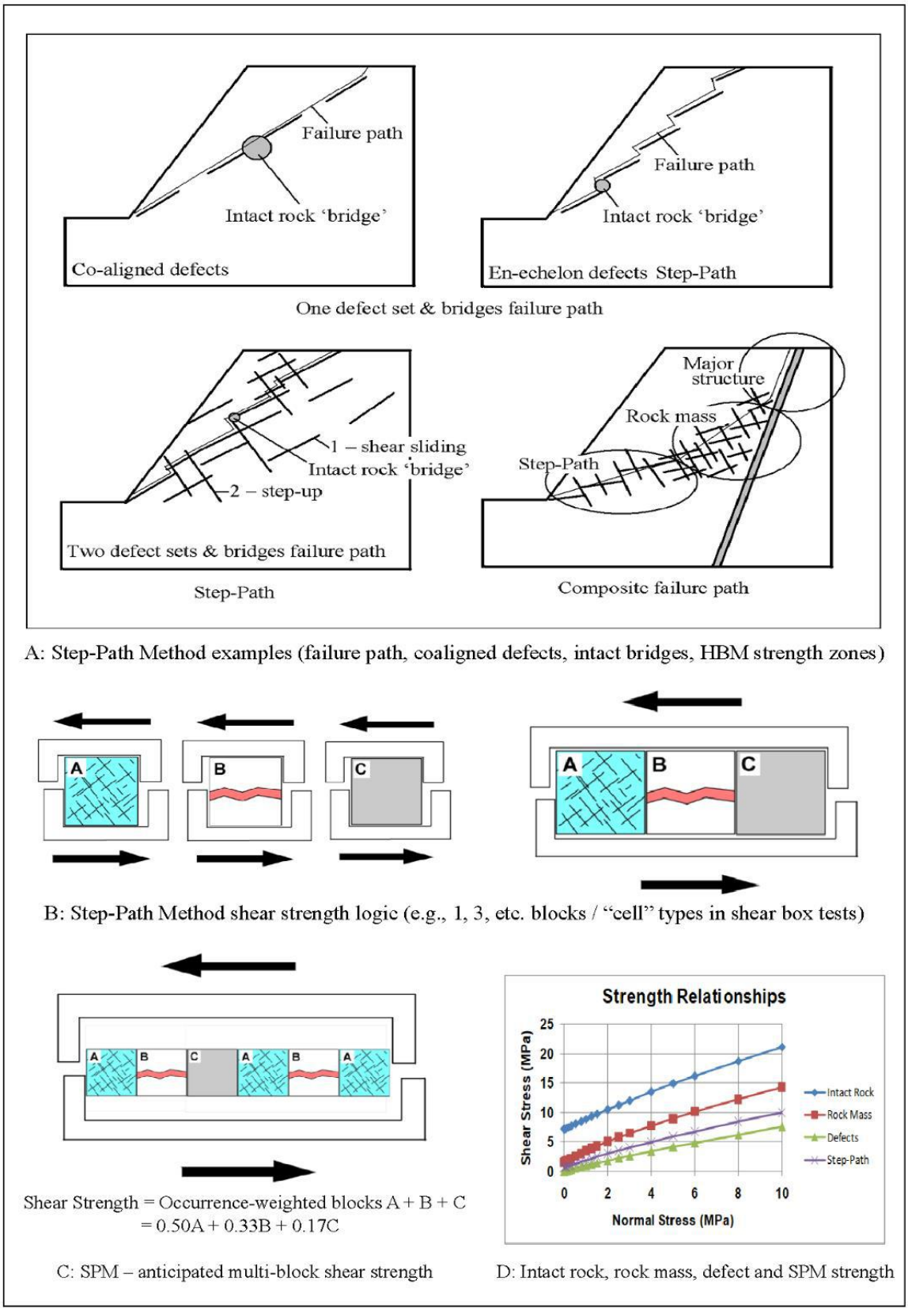

Figure 2: Step-Path model (Baczynski, 2019, 2022)

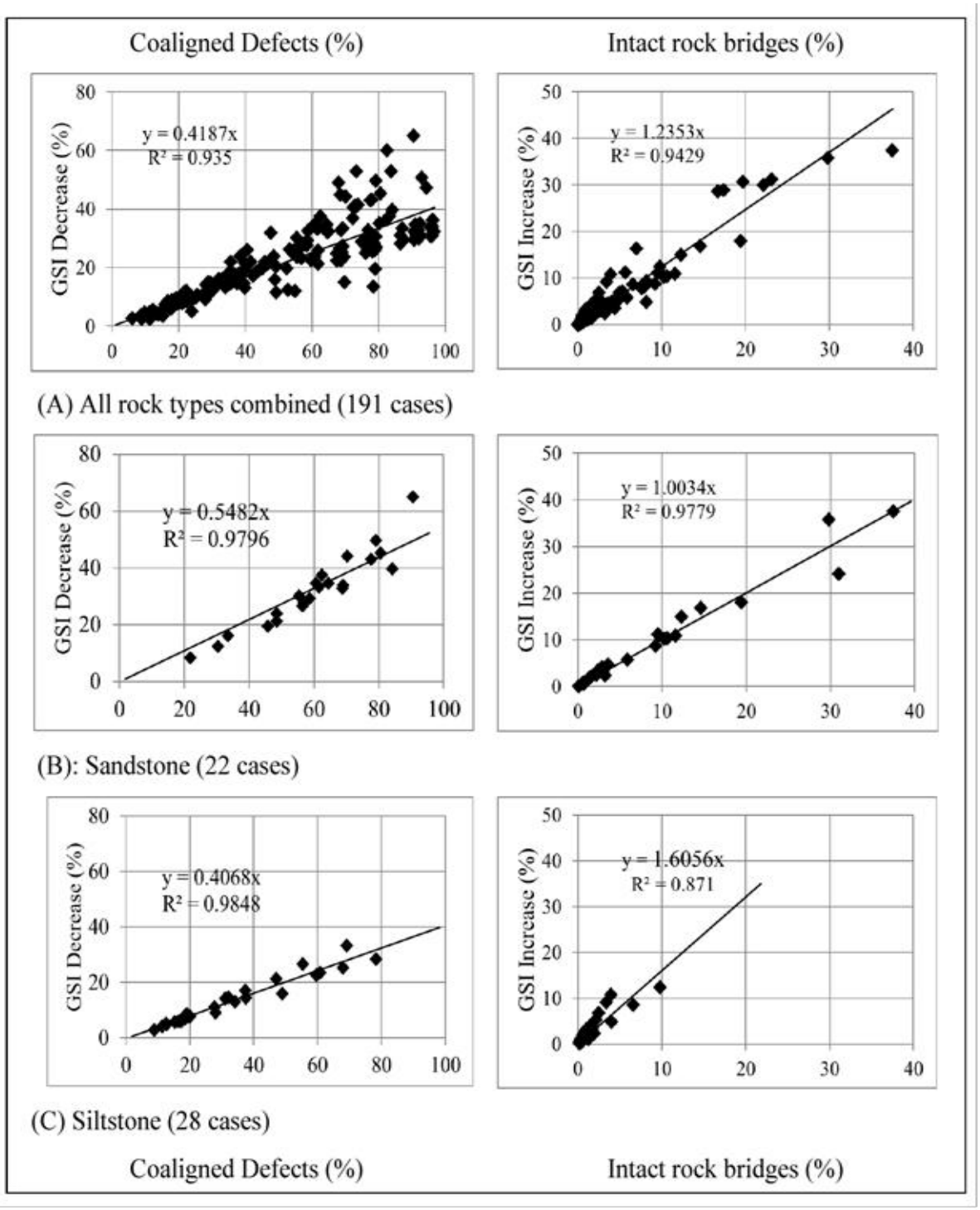

Figure 3: GSI adjustments (at 2 MPa normal stress) for relative occurrence of coaligned defects and intact rock bridges along failure paths through rock mass slopes (Baczynski, 2019)

6 MODEL SLOPE GEOMETRY

Various slope geometry models were considered, trialled and refined. Results in this paper are for 280m and 710m high slopes with overall face angles of 44°; as shown in Figures 4. Slope face in some models was vertically surcharged. This

was an attempt to simulate slope-scale direct shear tests and to reduce SRF from the often achieved >2 to ≤ 1.1. If applied, surcharge is flagged in this paper.

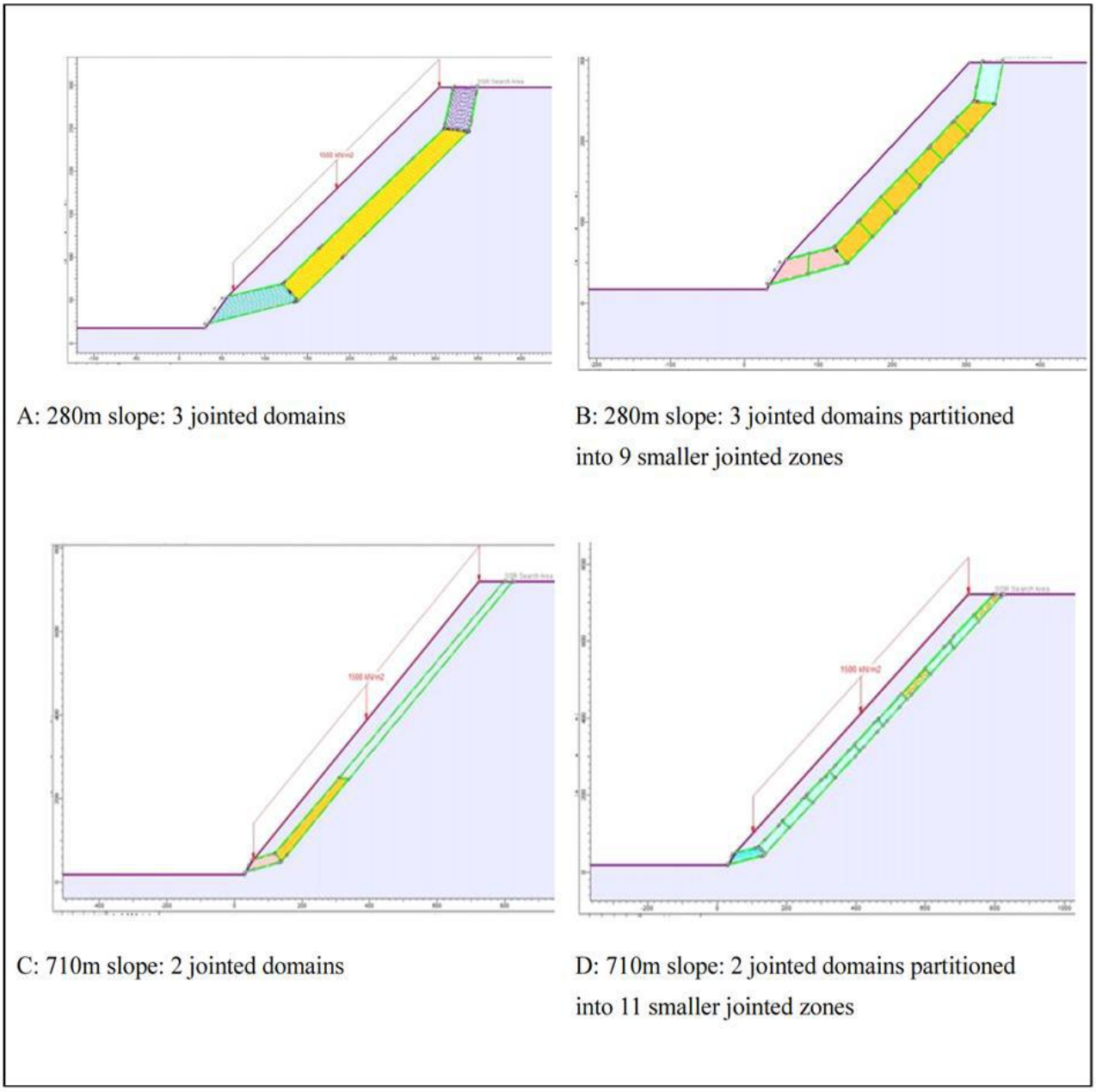

Figure 4: RS2 finite element slope models: jointed domains surrounded by unjointed rock mass

A 25m thick jointed area was located 30m behind the 280m high slope face. This area exited at slope toe and 30m behind slope crest. Ground on either side was unjointed. There were three joint-dip domains; each had one joint set. In the Upper, Central and Lower Domains joints dipped at 78°, 44° and 13° into the pit void, respectively.

Geometry of 710m high slope was similar to 280m high slope; but Central Domain was much longer. In most analyses, Upper Domain was deleted and Central Domain extended to ground surface.

With jointed domains, models broadly simulated slab-sliding conditions; with change in failure path trend at slab toe and in some models at slope crest. Nevertheless, this path is still similar to slip-circle failure with large radius and shallow depth traverse behind slope face.

In most analyses, three jointed "domains" were further partitioned into several shorter, each same length, jointed "zones". Such partitioning is akin to SPM concept of an assemblage of adjacent "cells" / blocks in Figure 2. As per Figure 4, there were 11 such jointed zones in 710m high slopes and 9 in 280m high slopes.

7 COALIGNED DEFECTS

Probability of occurrence, defect and bridge lengths and spacing between coaligned defect lines are discussed.

7.1 OCCURRENCE

Relative occurrence of coaligned defects in a rock mass may range between 0 and 100%.

"Joint-Ratio" setting in Joint Properties of RS2 software designates defect occurrence in each Jointed Zone. For comparison of RS2 results, a 0.8 "joint ratio" was usually used. Thus, if defects occurred in every jointed zone along slope failure path; defect occurrence was 80%. If a defect occurrence of 90% needed to be modelled, then the "Joint-Ratio" could be reset to 0.9.

In simplest models, all defects in specific jointed zones could be just deleted to reduce defect occurrence along failure paths. For example, with 0.8 joint ratio, each of the 9 jointed zones in the 280m high slope contained 80/9 = 8.9% of the coaligned defects. If defects were deleted in 3 of 9 zones, then 80 – 8.9 x 3 = 53.3% coaligned defects existed along the failure path. This approach was used to FE model the conceptual mean sandstone 2019 case study.

Coaligned defect occurrence in 2019 case studies was derived by slope face mapping. This value was rarely a convenient multiple of 8.9% occurrence in each of 9 jointed zones. Such situations were accommodated by dividing field occurrence by 8.9 to determine how many of the 9 jointed zones needed to contain defects in them and adjusting length of one zone to achieve the desired outcome. For example, a 56% mapped occurrence equates to 56/8.9 = 6.3 jointed zones. In this situation, length of one zone was increase by 0.3 (reducing the adjacent zone to 0.7 of its original length). Coaligned joints were assigned to 5 zones, plus the zone with 0.3 increased length. This resulted with joints in 6.3 zones and HBM rock mass strength (without joints) in the other 2.7 zones.

7.2 LENGTH

Figure 5 shows the mean defect length statistical model for 33 of the 230 Baczynski (2019) case studies that were RS2 modelled. Median and mode lengths are ~3m; this length was adopted

EXCEL-ROCLAB simplified SPM only considers cumulative lengths of each component (i.e., coaligned defects, intact rock bridges, rock mass bridges, HBM rock mass areas without coaligned defects) to compute shear strength.

In the original Step-Path STEPSIM Monte-Carlo simulation software (McMahon, 1979) and revised STEPSIM4 (Little et al, 1996-2000; Baczynski, 2000) coaligned defect length was a key input. Statistical models were based on field mapping and laboratory test data for defect type (fault, joint) and its occurrence, length, shear strength, cutoff probability by other defect sets, intact rock and rock mass "bridge" length for not cut-off defects and shear strength of these bridges. STEPSIM4 simulated 5,000 to 15,000 step-paths to develop failure path shear strength model.

7.3 ROCK MASS BRIDGES AND COALIGNED DEFECTS LINE SPACING

Length of rock mass (RM) bridges between coaligned defects is related to defect length and joint ratio. For example, with joint ratio of 0.8 and constant 3m defect length, RM bridge length is 0.77m. If defect length is increased to 5m, 10m, or 20m; respective RM bridge lengths increase to 1.3, 2.55 and 5.2m. Spacing between multiple lines of coaligned defects was purposely made same as RM bridge length. This approach ensured that slope failure path was not unintentionally restricted to traversing along a specific line(s) of coaligned defects (i.e., if bridges between the lines were longer), but was able to freely develop across multiple lines.

It perhaps worth noting that rock mass RQD with modelled bridge lengths and joint-line spacing is 100%. Hence, modelled defects in present finite element analyses do not impact "blockiness" rating along vertical axis of GSI Index charts. In this instance, often-cited perception that GSI rating should be somehow increased in HBM model to compensate for defects that are seemingly being considered twice lacks substance.

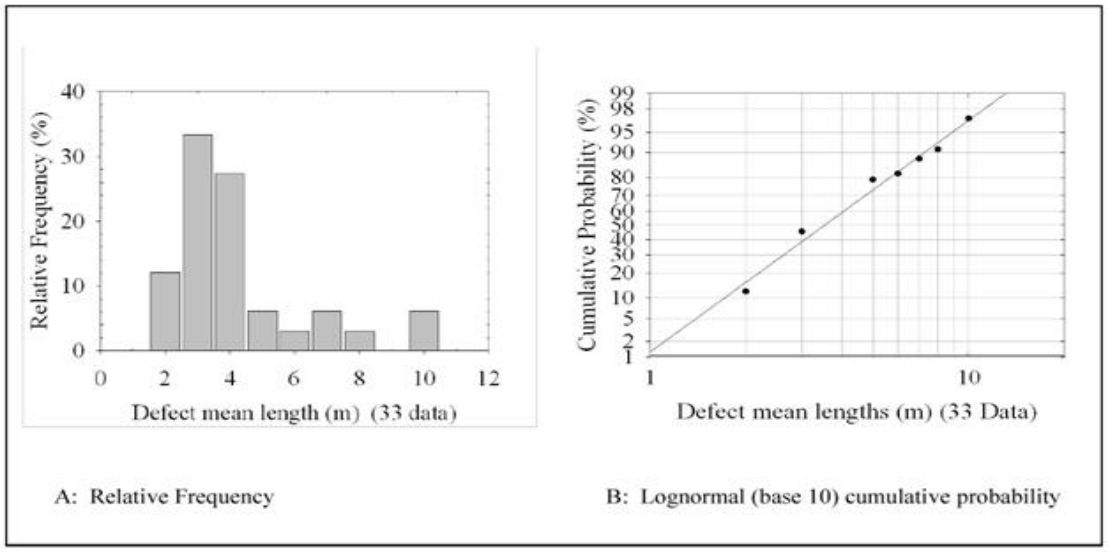

Figure 5: Mean sandstone and siltstone defect mean lengths in 2019 SPM case studies RS2 analysed

8 ROCK MASS AND DEFECT GEOTECHNICAL PARAMETERS

Table 1 details the range of rock mass and geological defect parameters that were considered in RS2 two-dimensional (2D) jointed finite element (FE) models. The Bandis-Barton model for joint shear strength was adopted (Barton, 1976, 2018; Barton and Bandis, 1990, 2017)

Table 1: RS2: Rock Mass and Defect Geotechnical Parameters

A: Hoek-Brown Rock Mass Strength						
Model	**Rock UCS (MPa)**	**GSI**	**mi**	**D**	**Young's Modulus (E) (GPa)**	**Poisson Ratio**
Conceptual Sandstone	30	60	17	0	250 x UCS 7.5	0.18
Sandstone 22 Cases	15-49	42-78	17	0	250 x UCS 3.8 – 12.3	0.18
Siltstone 11 of 28 Cases	25-100	35-65	7-15	0	250 x UCS 6.3 – 25.0	0.18
B: Geological Defects: Bandis-Barton shear strength						
Model	**JCS (MPa)**	**Roughness (JRC)**	**Base Friction $Ø_b$**	**Length (m)**	**Joint Stiffness (GPa/m)**	
					Normal	**Shear**
Conceptual Sandstone	30	6	30	3-20	4GPa: 1 case, otherwise 0.1	4GPa: 1 case, otherwise 0.01
Sandstone 22 Cases	15-49	5-11	30-32	3	0.1	0.01
Siltstone 11 of 28 Cases	25-100	4-8	29	3	0.1	0.01

9 STRESS REGIME AND STRENGTH REDUCTION FACTOR

Vertical stress is hydrostatic based on intact rock density of 24 kN/m3. Whilst the Poisson's Ratio is stated as 0.18; horizontal stress in finite element analysis was same as vertical stress.

RS2 finite element analyses specifically computed the SRF for jointed material domains only.

10 GSI ADJUSTMENT CALCULATIONS

This is a four steps process. Firstly, compute the strength reduction factor (SRF) for the model with joints. Then, repeat analysis for the model without joints. Aim is to determine the GSI reduction needed for the unjointed model to yield same SRF as the jointed model. The steps are:

Step-1: Do RS2 analysis for the candidate slope with the required HBM rock shear strength (say, UCS=30; GSI=60; mi=17; D=0) and required occurrence (say, 56%) of coaligned defects in jointed zones. Outcome depends on both HBM and joint shear strengths. Say, this yields SRF=1.53

Step-2: Redo RS2 analysis without coaligned defects in jointed zones. Outcome only depends on HBM shear strength (i.e., same inputs as indicated in Step-1). Say, this yields SRF=1.78

Step-3A: Redo Step-2 RS2 analysis but with GSI=60 reduced to GSI=50. Say, this yields SRF=1.68. This is higher than SRF=1.53 in Step-1

Step-3B: Redo Step-2 RS2 analysis but with GSI=60 reduced to GSI=40. Say, this yields SRF=1.58. This is still higher than SRF=1.53 in Step-1

Step-3C: Redo Step-2 RS2 analysis but with GSI=60 reduced to GSI=30. Say, this yields SRF=1.48. This is now lower than RS2 Step-1 result of 1.53.

Step-4: By further RS2 analyses within GSI=31 to GSI=39 range establish GSI value in the unjointed model that yields SRF=1.53; same as the SRF in Step-1. Alternatively, interpolate existing RS2 analysis result to reach same conclusion. In this example, SRF outcome for the jointed model in Step-1 is achieved when GSI=35 (and, UCS=30, mi=17, D=0) in the same model but without any coaligned joints in the jointed zones.

Step-5: Calculate the GSI adjustment; i.e., 60-35 = 25

11 FINITE ELEMENT RESULTS

Figures 6 to 10 summarize RS2 jointed finite element results.

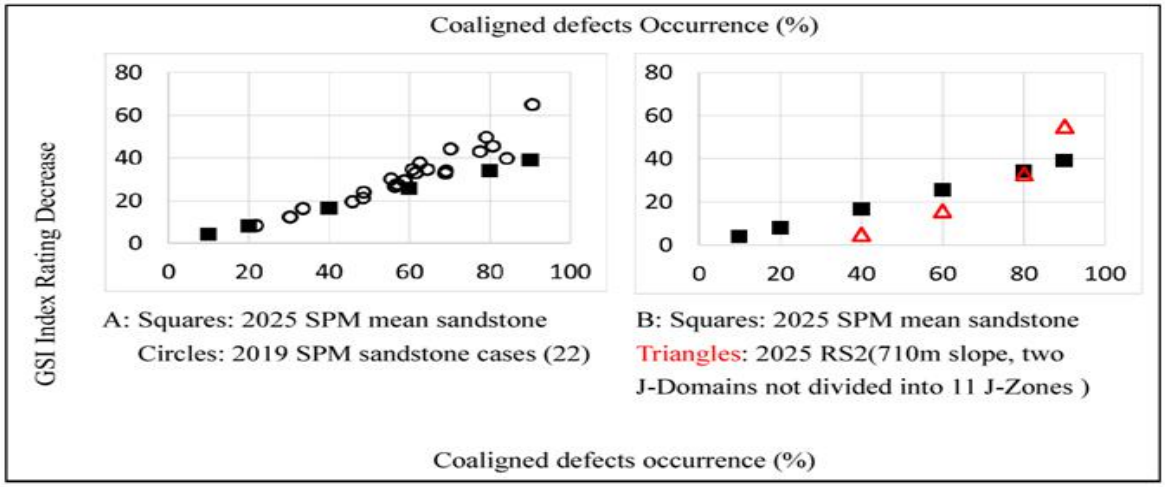

Figure 6: RS2 finite element results for 2025 SPM mean sandstone case study

11.1 STEP-PATH METHOD LOGIC CHECK

Initial FE analyses checked validity of SPM logic. A mean conceptual sandstone model (see inputs in Table 1) was tested over 10-90% coaligned defect occurrence range. Black circles in Figure 6A are actual Baczynski (2019) results for 22 sandstone case studies (as derived by EXCEL-ROCLAB calculations); black filled squares are 2025 likewise-derived results for mean sandstone test model.

As per Figures 4A and 4C, 280m and 710m high slope models each initially had three jointed domains. Joints in Upper, Central and Lower Domains dipped at 78^o, 44^o and 13^o towards pit void, respectively. In subsequent 710m slope models, Upper Domains was abolished and Central Domain extended to ground surface. The red triangles in Figure 6B are RS2-derived GSI adjustments for 30-90% coaligned defect occurrence in the two jointed domains of 710m slope model. Whilst a match exists between SPM-predicted and RS2-achieved GSI adjustments at 80% coaligned defect occurrence, RS2 analyses indicate lower GSI-adjustments for lower coaligned defect occurrences; trending to 0% GSI adjustment below 30% coaligned defect occurrence. RS2 re-analyses of the same models with much reduced Mohr-Coulomb joint shear strength inputs failed to significantly alter the overall outcome.

On reflection, initial FE analyses were not honouring the Step-Path concept in Figure 2. Defects of particular defect set tend to occur in clusters / zones (Baczynski, 1980 a, b).

Extent of clusters in directions parallel and normal to a defect set's mean plane may be defined in terms of conditional probabilities (i.e., the greater the intensity of the defect set in a "cell", the greater the likelihood that immediately adjacent cells will also have high intensity and vice-versa). It is worth noting that if defects were randomly distributed, line-sampled defect spacing would not be lognormal. The SPM rock mass model conceptually comprises an array of adjacent relatively small size "cells" which may have 1 or more through-going coaligned defects in each cell. Defect occurrence is simply estimated by partitioning line traverse slope face mapping data into 5m or 10m segments (or akin 5m x5m or 10m x 10m mapping windows) and determining how many line-segments / mapping windows contain specific defect sets in them.

Figures 4B and 4D show that the SPM "cells" concept was achieved in RS2 models by partitioning the 2 jointed domains in 710m high and 3 jointed domains in 280m high slopes into 11 and 9 smaller jointed "zones", respectively. Partitioned jointed "zones" were used in all subsequent RS2 analyses.

11.2 SINGLE-LINE VERSUS MULTI-LINE COALIGNED DEFECTS

Figure 7 shows GSI adjustment outcome for models with single-line and multi-lines of coaligned defects. Multiline RS2 model yields similar results to SPM. Single-line results are 60-70% less.

11.3 COALIGNED DEFECT LENGTH IMPACT

Figure 8 shows RS2 analysis GSI adjustments for multiline models with 3m long coaligned defects and 0.77m rock mass bridges and line spacing and with 10m long defects and 2.55m bridges / line-spacing. GSI adjustments for shorter defects and bridges are similar to somewhat higher than SPM predicted; those for longer defects are generally less, especially for defect occurrences > 60%.

11.4 RS2 ANALYSIS OF 2019 SPM CASE STUDIES

Twenty-two (22) sandstone and 11 siltstone of Baczynski (2019) case studies were RS2 modelled. Results are shown in Figures 9 and 10.

In spite of the data scatter in Figures 9A and 9B, there is good agreement between 2019 SPM-predicted and 2025 RS2-achieved GSI adjustments for sandstone and siltstone case studies. The two linear trend lines coincide in Figure 9B.

Figures 9C to 9E plot the respective results for sandstone case studies without and with the cases being partitioned with respect GSI (i.e., GSI>73 and GSI<74). Half of sandstone cases were for GSI>73. This GSI is near upper limit of Baczynski (2019) GSI adjustment equation's application. After partitioning, RS2 analyses of GSI<74 group (Figure 11D) achieved a reasonable match with 2019 SPM-predicted results. In GSI>73group, SPM predicted higher GSI adjustments than RS2 modelling.

11.5 JOINT STIFFNESS IMPACT ON RS2 RESULTS

Joint normal and shear stiffness testing data was not available for any of the 230 Baczynski (2019) case studies. Such data is rarely collected during routine geotechnical investigations and was not an input to HBM and SPM analyses. A large volume of literature exists on joint stiffness but values vary considerably between authors. Papers include Bandis et al (1983), Moorzad and Aminpoor (2008), Kulatilake et al (2016), Han et al (2023), Niktabar et al (2023) and Wang et al (2024). As per Table 1, 0.1 GPa/m and 0.01 GPa/m were adopted for normal and shear defect stiffness. Only one suite of RS2 analysis was done with joint stiffness increased up to 4 GPa/m. With stiffer defects, the RS2 computed SRF increased by 5-10%.

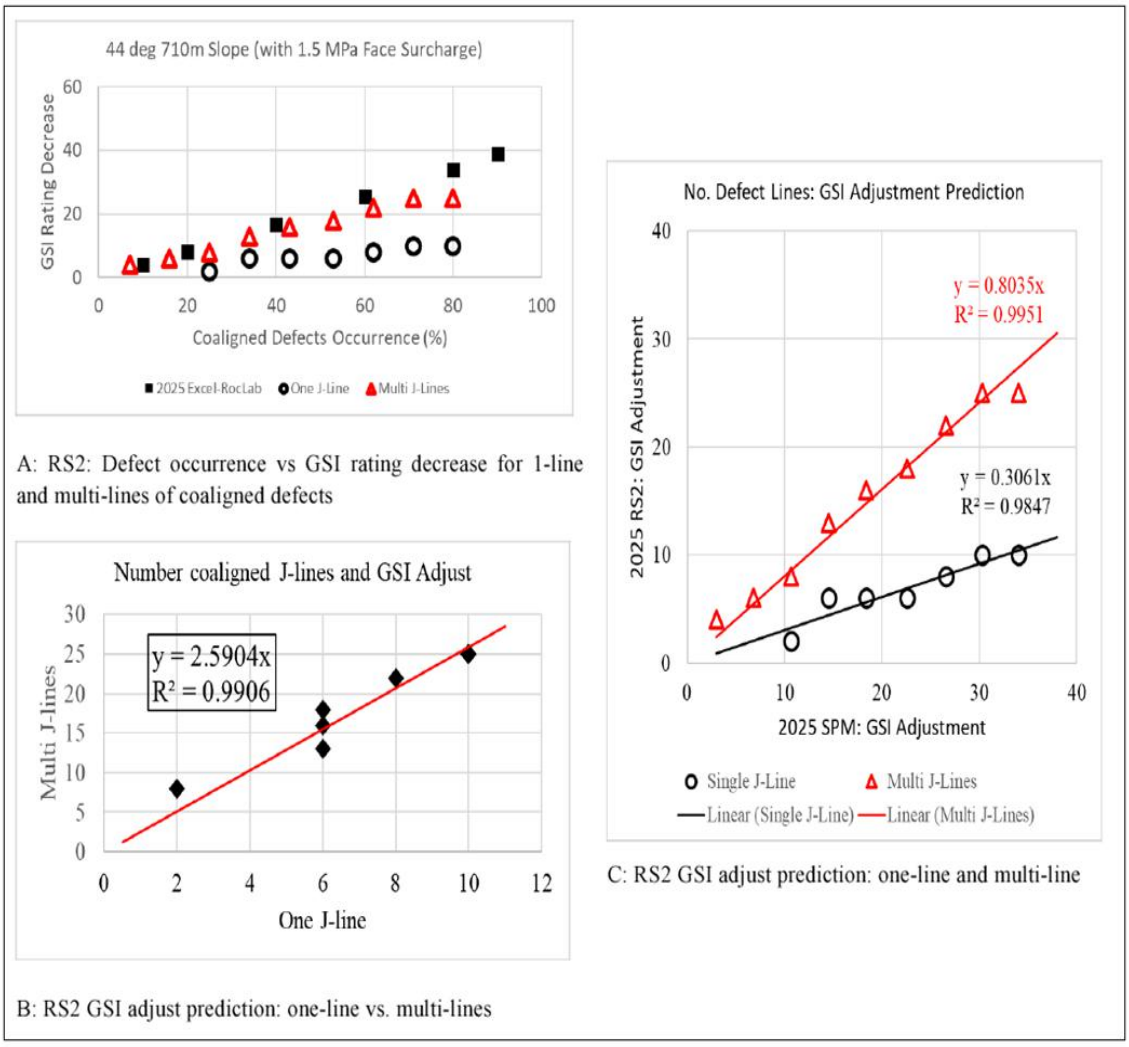

Figure 7: 2025 SPM mean sandstone: RS2 derived GSI adjustments for one and multi-lines of co-aligned defects

11.6 2019 SPM VERSUS 2025 RS2 GSI-ADJUSTMENT PREDICTION

Figures 10A to 10F indicate that RS2 finite element analyses have confirmed SPM logic for predicting GSI-Adjustments in HBM rock masses for GSI <74 situations. Correlation coefficients for sandstone and siltstone trendlines in Figures 10B, 10E and 10F are 0.92, 0.91 and 0.98; respectively.

In view of various factors (e.g., number of lines of coaligned defects, defect length and defect stiffness, and also likely the number of smaller joint zones partitioning larger jointed domains) that had been shown to impact RS2 modelling outcomes, there has been a fairly strong confirmation of Baczynski (2019) SPM logic and GSI adjustment equations

reconciling SPM and HBM rock mass strength estimates. This GSI adjustment model applies to those defects that are significantly coaligned with the failure path through the rock slope; with sliding into the excavation direction.

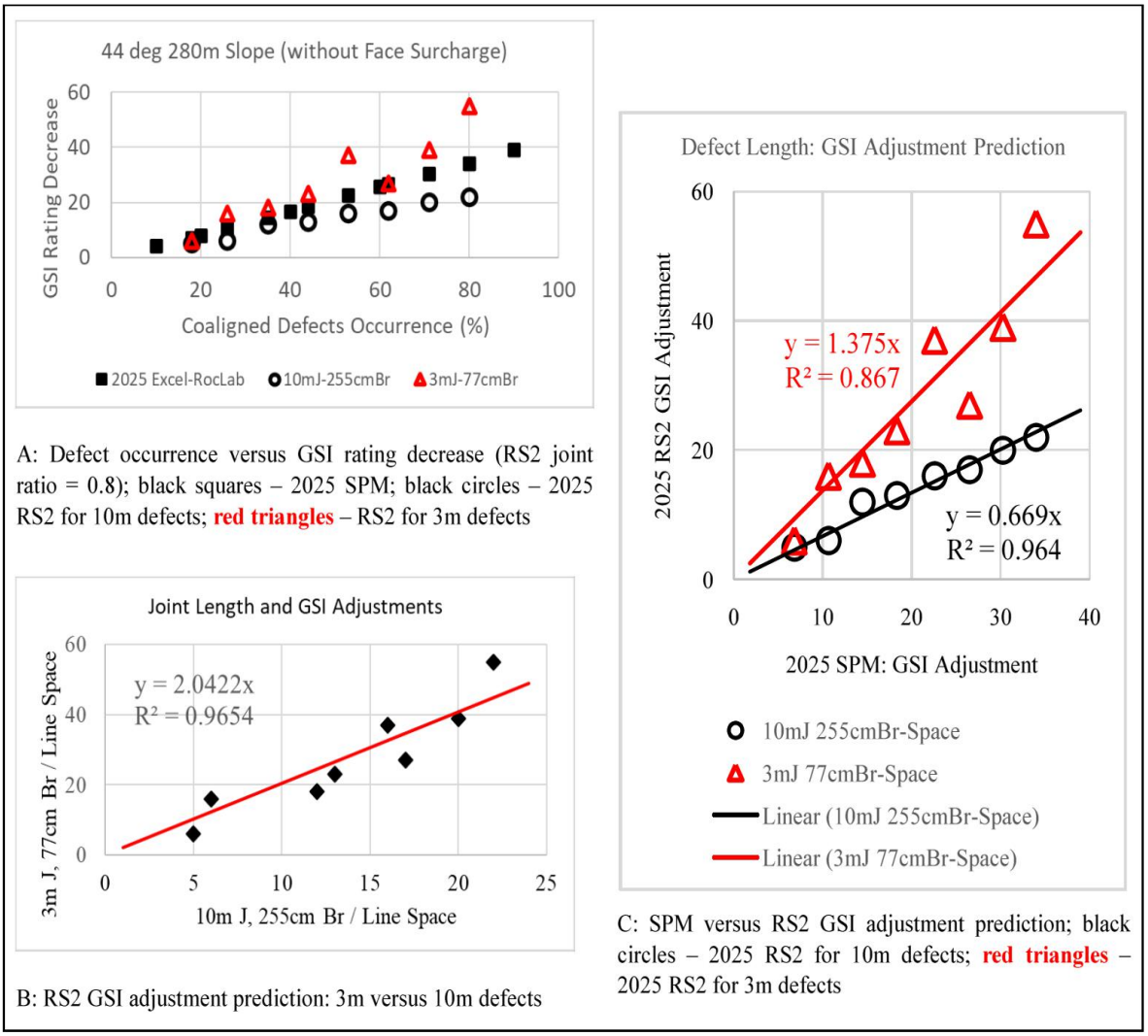

Figure 8: 2025 SPM mean sandstone: RS2 derived GSI adjustments for multi-lines of 3m and 10m long defects

11.7 NON-LINEARITY OF GSI MODEL

Figure 11 best explains the reason for the upper GSI limit stated in Baczynski (2019) GSI-adjustment equation. In Figure 11A, spacing between shear strength curves increases with increasing GSI. In the 1-3 MPa normal stress range that likely exists in many shallow-seated rock slope failures, spacing between the plotted curves is fairly similar up to GSI~70; but widens significantly for higher GSI values.

This normal stress impact above 3 MPa is again highlighted in Figure 11B. Figure 11C and 11D closer examine this matter. The GSI vs shear strength trend is linear for GSI<70; then there is non-linear transition between GSI=70-90; and perhaps a linear trend at GSI>90. Baczynski (2019) had suggested that perhaps the GSI trend could be considered in terms of two linear relationships, somewhat as shown in Figure 11D; with the transition point at about GSI=75. But this consideration was not further pursued. It suffices to note that the present RS2 finite element analyses infer that 2019 published GSI adjustment equations may overestimate GSI adjustments for coaligned defect occurrence in rock masses with GSI>72, and that the cut-off limit for SPM GSI adjustments should perhaps be somewhat reduced from the published GSI=75 to perhaps GSI=72 or 73.

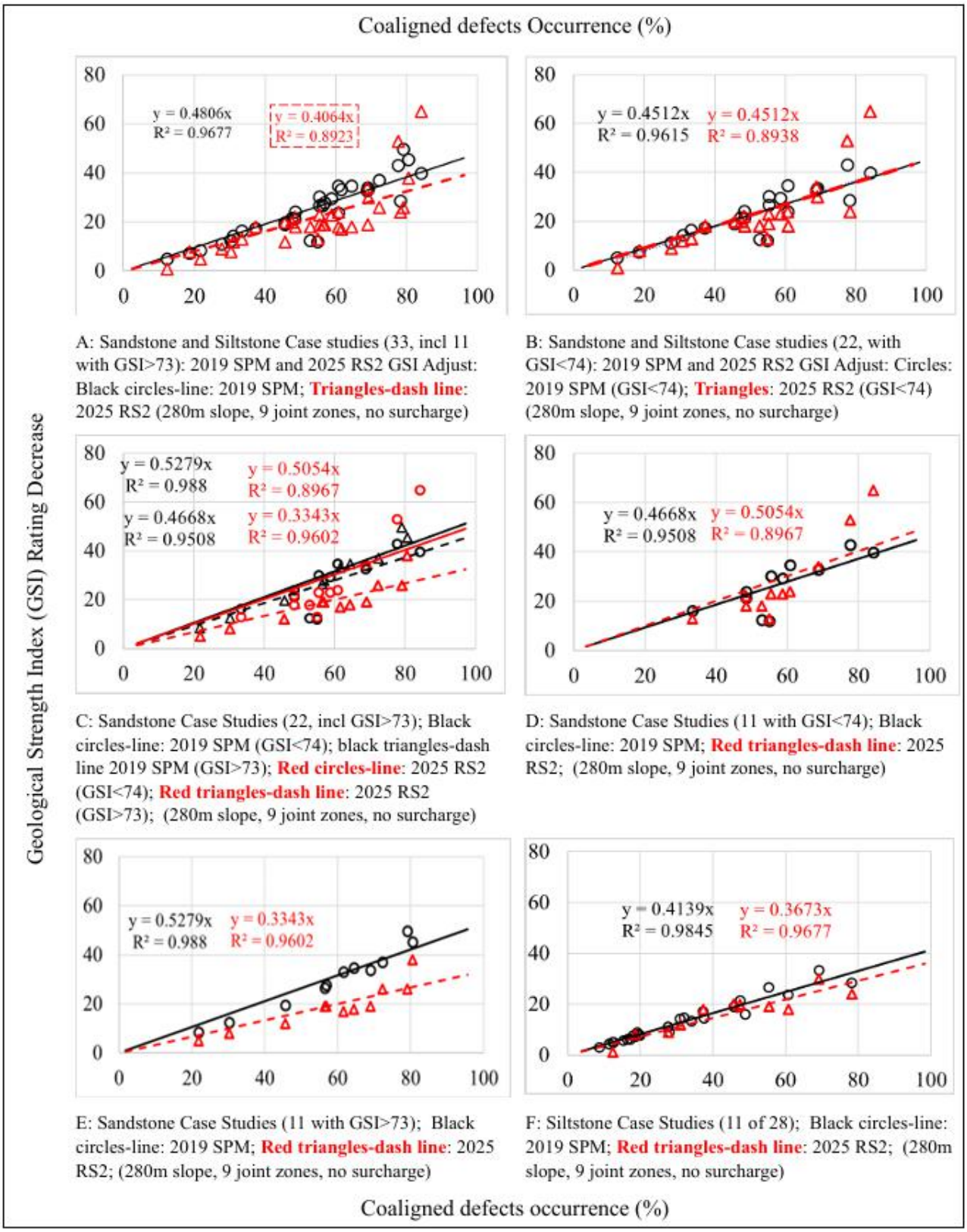

Figure 9: RS2 finite element results for 2019 SPM sandstone and siltstone case studies

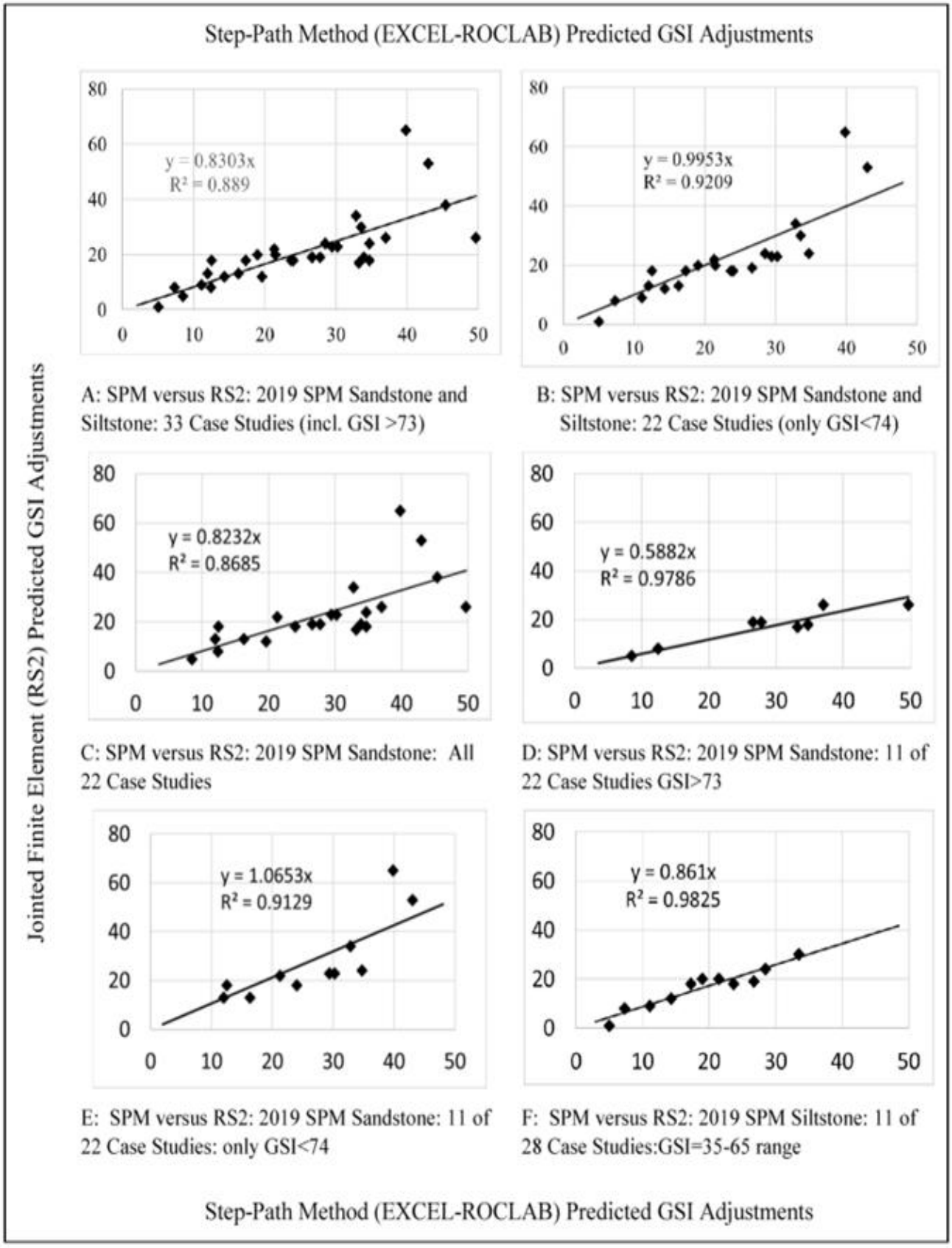

Figure 10: Step-Path Method versus RS2 finite element predicted GSI Adjustments

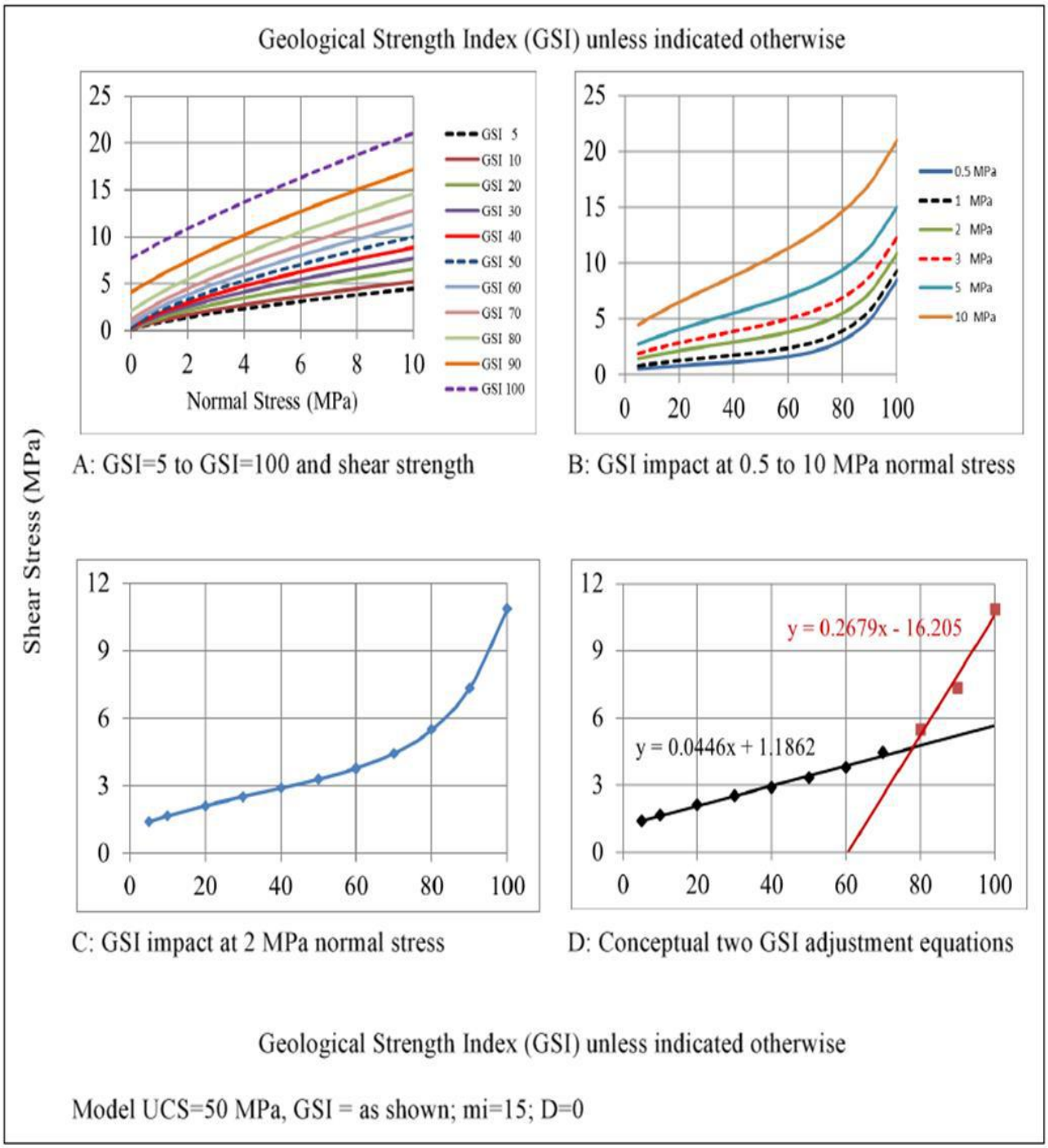

Figure 11: Shear stress outcome due to non-linearity of GSI Index model (Baczynski, 2019)

12 DISCUSSION

The GSI adjustment equation comprises two parts. Firstly, there is a negative GSI adjustment for the relative occurrence of geological defects that are coaligned with slope failure paths. Secondly, there is a positive GSI adjustment for the relative occurrence of intact rock bridges between the coaligned defects. Finite element modelling presented in this paper checked the coaligned defects component. All modelled bridges were rock mass strength. Validation of intact rock bridges is still required.

Completed RS2 analyses assessed two model types. The first was a near-mean conceptual sandstone model; second comprised all of the 22 sandstone and 11 of 33 siltstone case studies in Baczynski (2019).

Conceptual models aimed to broadly check the validity of negative GSI adjustments logic and to understand how various factors impacted outcomes. Factors included single and multiple lines of coaligned defects along failure paths, defect occurrence in clusters (zones), length, rock mass bridge lengths (and line spacing) between them, shear strength and normal / shear stiffness. Irrespective of their potential numerical modelling importance, defect stiffness and rock mass dilation are not inputs to GSI index in the HBM. Hence, these should not be deemed additional constraints to be considered in reconciling SPM and HBM strengths via GSI adjustments.

Slope face of some models was 1.5 MPa vertically surcharged to achieved 2-3 MPa normal stress on dipping defect surfaces and thus provide results in same stress range as considered in Baczynski (2019). Results are summarized in Sections 11.1 to 11.5.

Figures 9 and 10 and Sections 11.6 summarize the results of 2019 case study FE modelling. Initial intention was to just FE model all of the 22 sandstone cases to check validity of 2019 GSI adjustment equation. Eventually, 11 siltstone cases were also modelled. The selected siltstone subset aimed to have FE results over the full range of coaligned defect occurrences (10% to 80%) and to consider siltstone from several locations.

13 FUTURE NUMERICAL MODELLING

To date, 33 of the 230 case studies in Baczynski (2019) had been FE modelled. Ideally, the rest or at least a greater number of these cases should likewise be modelled.

In real rock masses, not all defects are perfectly coaligned with failure paths. As coalignment decreases, the negative GSI adjustment will likewise decrease. It is anticipated that this GSI decrease will likely resemble the Snowden adjustment that already exists in the RS2 software (Rocscience, 2020). There's an opportunity to check this situation with the already created RS2 models.

The positive GSI adjustment impact of intact rock bridges between coaligned defects has not been FE checked. This work is required to fully validate the 2019 published GSI adjustment equation. Presently considered rock mass bridges were 0.77 to 5.2m long. Intact rock bridges are typically very much shorter (often 0.01 to 0.3m) and rarely exceed 1m. A new suite of FE models will be required to assess intact rock bridges.

14 CONCLUSIONS

Coauthors conclude that two-dimensional, jointed RS2 finite element analyses had overall verified the Step-Path Method logic and approach of negative GSI adjustments in Hoek-Brown Method for coaligned defect occurrence along failure paths in rock slopes. Coaligned defects are those that near-parallel the failure path trend and dip into the pit excavation. The positive GSI adjustment impact of intact rock bridges between coaligned defects remains to be FE checked.

Baczynski (2019) GSI-adjustment equation adjustments are valid for rock masses with GSI $\leq$ 73; this upper-bound GSI is marginally less than originally suggested, where co-aligned defects dip into the excavation.

Before using these GSI-adjustment equation(s), the analyst should check that the process is not confounded by joint shear strength exceeding Hoek-Brown rock mass strength.

Defect shear strength curve should not cross over the Hoek-Brown rock mass shear strength curve within the normal stress interval (say 1-3 MPa) of slope stability analysis interest. Geotechnical inputs to HBM and Bandis-Barton shear strength analysis equations are not identical. Hence, strength curve cross-overs may occur for low mi and low UCS in HBM equation and for moderate to high JRC and JCS values in Bandis-Barton equation. In reality, geological defects are rarely stronger than rock masses, apart from situations where the rock is extremely weathered to decomposed and defects are very rough and strongly cemented (e.g., quartz, iron oxide).

15 ACKNOWLEDGMENTS

This jointed finite element analysis would not have been possible without Rocscience RS2 software being provided for an extended trial period. Time, assistance and patience of Jiwoo Ahn of Rocscience Australia are much appreciated.

16 REFERENCES

Baczynski, N.R.P. (1980a). Zonal Concept for Spatial Distribution of Fractures in Rock. *Proc. 3rd Aust. NZ Conf. Geomech.*, Wellington, New Zealand, 12-16 May 1980, Vol.2, pp. 2-29 to 2-33.

Baczynski, N.R.P. (1980b). Rock Mass Characterization and Its Application to Assessment of Unsupported Underground Openings. *PhD Thesis*, Department of Mining & Metallurgy, University of Melbourne, Vic., Australia, dated 25 Nov. 1980, 233p., 66 Figures, 15 Tables, Appendix 1 (5p.)

Baczynski, N.R.P. (2000). STEPSIM4 Step-Path Method for slope risks. *GEOENG 2000, Pro Int Conf Geotech & Engng. Geol*, Melbourne, Australia, 2, 86

Baczynski, N.R.P. (2018). Step Path adjusted Hoek Brown GSI Chart. *Proc. 10th Asian Rock Mech. Symp., ARMS10, The ISRM Int. Symp. 2018*, 29 Oct – 3 Nov, Singapore, 12p

Baczynski, N.R.P (2019). GSI adjustments for directional Hoek-brown strength calibrated by Step-Path case studies. *Aust Geomech J.*, 54(3), p51-78.

Baczynski, N.R.P (2022). Step-Path Method for rock slopes. *University of Queensland, Course UQ CIVL 4280, 2022 Advanced Rock Mechanics*, Guest Lecture, 15 Aug 2022, PPTX PowerPoint, 136 slides.

Bandis, S.C., Lumsden, A.C. & Barton, N.R. (1983). Fundamentals of rock joint deformation. *Int. J. Rock Mech. Min. Sci. Geotech. Abstracts,* 20(6), pp 249-268.

Bar, N. & Baczynski, N.R.P. (2019). Slope failure risks by engineering geological logic and the Simplified Step-Path Method. *13th Aust NZ Conf Geomechanics*, Perth, Australia, 5p.

Barton, N., Lien, R., & Lunde, J. (1974). Engineering classification of rock masses for the design of tunnel support. *Rock Mech.*, 6(4), pp 189-236

Barton, N.R. (1976). The shear strength of rock and rock joints. *Int. J. Rock Mech. Min. Sci. Geotech. Abstracts*, 13(9) pp 255-279

Barton, N.R. & Bandis, S.C. (1990). Review of predictive capabilities of JRC-JCS model in engineering practice. In *Rock Joints, Proc. Int. Symp on rock joints*, (ed. N. Barton and O. Stephansson), pp 603-610, Rotterdam, Balkema.

Barton, N.R. & S.C. Bandis, 2017. Characterization and modelling of the shear strength, stiffness and hydraulic behaviour of rock joints for engineering purposes. *Rock Mechanics and Engineering*, Ed. Xia-Ting Feng, Vol. 1, Ch. 1, pp. 3-40. Taylor & Francis.

Barton, N. (2018). Barton-Bandis Criterion. In Bobrowsky, P., Marker, B. (eds) *Encyclopedia of Engineering Geology*. Geology. Encyclopedia of Earth Sciences Series. Springer, Cham.

Bieniawski, Z.T. (1976). Rock mass classification of rock masses and its application in tunnelling. *Proc. Third Int. Cong. Rock Mech. ISRM*, Denver, 11A, 27-32.

Bieniawski, Z.T. (1989). *Engineering rock mechanics classification*. New York, Wiley.

Deere, D.U. (1963). Technical Description of Rock Cores for Engineering Purposes. *Rock Mech. Engng. Geol.*, Vol 1, pp.16-22.

Han, G, Chen, Z., Xiang, J., Gao, Y., Zhou, Y., Tang, Q. & Chen, W. (2023). Numerical simulation study on shear properties of rock joints under CNS boundary conditions. *Geotech. Geol. Engng.,* Vol 42, pp.1351-1371

Hoek, E. & Brown, E.T. (1980). Empirical strength criterion for rock masses, *ASCE J Geotech Div*, 106 (9), pp 1013-1035

Hoek, E. & Brown E.T. (1997). Practical estimates of rock mass strength. *Int J Rock Mech Min Sci*, 34(8), pp 1165-1186

Hoek, E, Carter T.G. & Diederichs, M.S. (2013). Quantification of the Geological Strength Index Chart. *Proc 47th US*

Rock Mechanics / Geomechanics Symp, 23-26 June 2013, San Francisco CA, USA.

Jennings, J.E (1970). A mathematical theory for the calculation of the stability of slopes in open cast mines. *Proc. Symp. Planning Open Pit Mines*, PWJ van Rensberg (ed), Johannesburg, Balkema (Cape Town, 1971), pp 87-102

Kulatilake, P.H.S.W., Shreedharan, S., Sherizadeh, T., Shu, B., Xing, Y. & He, P. (2016). Laboratory estimation of rock joint stiffness and frictional parameters. *Geotech. Geol. Engng.,* Vol 35, 13p.

Lambert, J. & Frye, C. (2022) Microsoft Excel (Office 2021 and Microsoft 365) Step-by-Step", Microsoft Corporation & Pearson Education, Inc., 67p

Little, T.N. Cortes, J.P. & Baczynski, N.R. (1997-2000). Risk-based slope design optimisation study for the Ok Tedi copper-gold mine. Vol 1 to 8 & Executive Summary, Ok Tedi Mining Limited, Mine, Technical Services Dept., Geotech. Engng. Section, internal report

McMahon, B.K. (1979). Report to Bougainville Copper Limited on slope design studies, Pan Hill, McMahon, Burgess & Yates, Sydney, internal report.

Niktabar, S.M.M.; Rao, K.S., Shrivastova, A.K., & Scucka, J. (2023). Effect of varying stiffness of rock joints under 0cyclic shear loads, *Materials,* Vol 16, No. 4272, 20p.

Noorzad, A. &, Aminpoor, M. (2008). Effect of joint stiffness values on stresses of jointed rock. *ISRM Int Symp 2008, Fifth Asian Rock Mech. Symp. (ARMS5),* 24-26 Nov 2008, Tehran, Iran, pp. 437-443

Rocscience (2007). Roclab 1.0, Users Guide, 19p.

Rocscience (2020). RS2: Slope Stability Verification Manual. Parts 1 to 4, 441p

Rocscience (2024). RS2: Joint Analyses Verification Manual. 108p

Truzman, M. (2007). Statistical summary of rock mass characterization for tunnels of the Caracas-Tuy Medio Railway Project", *Proc XXIII Pan-American Conf Soil Mech Geotech Engng*, Margarita Is, Venezuela, 2, pp 877-882

Wang, B., Jiang, Y., Zhang, Q., & Chen, H. (2024). Shear behaviour of intermittent joints subjected to shear cycles under constant normal stiffness conditions: effects of loading parameters. *J. Rock Mech. Geotech. Engng,* Vol 16 (2024), 43p.